RSC Advances

Cite this: DOI: 10.1039/c0xx00000x

www.rsc.org/xxxxxx

PAPER

Metallosalen-based microporous organic polymers: synthesis and carbon dioxide uptake

He Li[a], Zhongping Li[a], Yuwei Zhang[a], Xiaolong Luo[c], Hong Xia[b], Xiaoming Liu*[a] and Ying Mu[a]

Received (in XXX, XXX) Xth XXXXXXXXX 200X, Accepted Xth XXXXXXXXX 200X

DOI: 10.1039/b000000x

This article describes the synthesis and carbon dioxide uptake of new organic microporous frameworks with built-in metal sites in the skeleton. Three novel microporous polymers have been synthesized via a Sonogashira-Hagihara coupling reaction with 1,3,5-triethynylbenzene and diverse metallosalen building blocks. These materials are insoluble in conventional solvents and exhibit high thermal and chemical stability. According to the nitrogen physisorption isotherms, the highest Brunauer-Emmett-Teller specific surface area up to 1200 m^2 g^{-1} was obtained for three polymer frameworks with a pore volume of 0.94 cm^3 g^{-1}. The polymer frameworks display high carbon dioxide uptake capacities (up to 8.2 wt%) and good selectivity at 273 K and 1 bar, which impacted significantly by the porosity of the frameworks, active heteroatoms and coordinatively unsaturated metal sites in the skeletons.

Introduction

The emission of CO_2 from fossil fuel combustion is the major contributor to global-warming.[1] The development of new technologies and methods for CO_2 capture and sequestration is necessary. Porous materials such as zeolites, activated carbon, alumina and metal-organic frameworks (MOFs) have been proposed as potential CO_2 sorbents due to the high surface areas and isosteric heat of CO_2 adsorption.[2] In recently year, microporous organic polymers (MOPs) including solution-processable polymers of intrinsic microporosity (PIMs),[3] hypercross-linked polymers (HCPs),[4] conjugated microporous polymers (CMPs),[5] covalent triazine-based frameworks (CTFs)[6] and covalent organic frameworks (COFs)[7] have been attracted considerable attention as a new class of porous materials, and showed great potential applications in fields such as gas storage and separation,[8] chemical sensor,[5c,9] and heterogeneous catalysis.[10] Compared with traditional inorganic microporous materials, organic porous polymers possess a number of advantages. For example, MOPs are mainly constructed from organic molecules through strong covalent bonds and have been demonstrated to be air and moisture stable, the skeleton totally composed solely of the light elements (C, H, O, B and N) and possess quite high gas storage capacity. In addition, one of the most attractive aspects is the promise of tuning structures, properties and functionalities through rational chemical design, synthesis methods and intensive selection of organic building blocks. Many MOPs have been demonstrated as promising materials for CO_2 store.[8] The CO_2 adsorption of MOPs depends not only on the surface area or the pore size, but also on the chemical composition of the materials.[11] An effective strategy to improve the adsorption capacity for CO_2 is to introducing special active sites such as heteroatom and diverse organic functional group into the polymer frameworks to increase the interactions between adsorbent and CO_2.[12] For example, several Nitrogen-containing materials have been confirmed as excellent adsorbents for CO_2 adsorption.[13] Organic functional group such as amine, carboxylic acid and hydroxyl incorporated to porous organic frameworks can increase the CO_2 uptake in low pressure.[12b,14] For example, Zhu's group has reported that introduction of light metal ions can improve the adsorption affinity to CO_2.[15] Recently, Gumma and coworkers demonstrated the various coordinatively unsaturated metal cations of the DOBDC series of MOFs have impact on the adsorption of CO_2.[16] However, the gas storage properties of microporous organic polymers with varying built-in unsaturated metal sites in the skeleton have rarely been explored.

Shiff-base salen is a class of interesting tetradentate ancillary ligand with a rich coordination chemistry and their corresponding metallosalen complexes are excellent catalysts for a lot of molecular transformations and polymerization reactions.[17] Up to now, to the best of our knowledge, only a few examples of porous materials containing metallosalen units were reported.[18] In sharp contrast with metallophthalocyanine and metalloporphyrin, metallosalen units as building blocks for MOPs possess some significant advantages, such as facile synthesis, high yield, convenient to adjust the spatial and electronic structure. With these considerations in mind, we report herein on a series of metallosalen-based microporous organic polymers (MsMOPs). These MsMOPs possess unique microporous characters with high BET surface areas, large pore volume, good stability, and as well as display good adsorption capacity for CO_2. We also suggest the differently unsaturated metal sites in the skeletons impact their porosity and CO_2 uptake.

Results and discussion

Using metallosalen and 1,3,5-triethynylbenzene as comonomers, three metal functional microporous organic polymer frameworks were synthesized by the Sonogashira-Hagihara palladium catalyzed cross-coupling reaction (Scheme 1). As an example of MsMOP-Ni, we investigated the different solvent systems including toluene/triethylamine (TEA), dioxane/TEA, *N,N*-dimethylformamide (DMF) /TEA and tetrahydrofuran (THF)/TEA in the polymerization reactions, in order to achieve high surface areas for the resulting polymer frameworks. As an optimal condition, polymerization reaction carried out in THF/TEA (1/1 in volume) using $Pd(PPh_3)_4$/CuI as catalyst, MsMOP-Ni with the largest surface area can be prepared. Under the same reaction conditions, we further synthesized MsMOP-Zn and MsMOP-Pt with large surface areas and different Lewis metal sites in the skeleton.

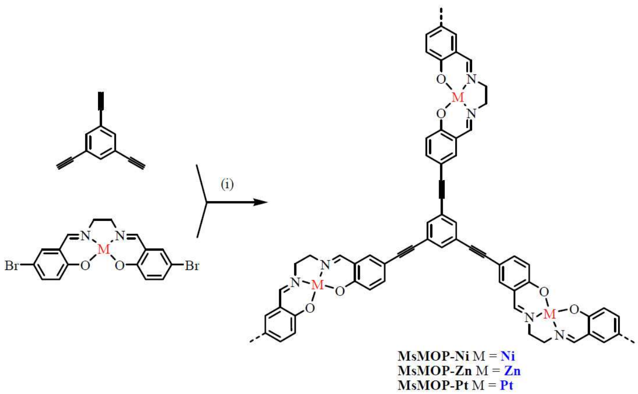

Scheme 1. Synthetic procedure of metallosalen-based microporous organic polymers using (i) THF/NEt_3, $Pd(PPh_3)_4$, CuI, 80 °C, 72 h.

MsMOPs are insoluble in common organic solvents such as hexane, ethanol, acetone, THF or DMF. Thermogravimetric analysis (TGA) under nitrogen demonstrated that these metallosalen based microporous polymer networks have high thermal stabilities (Fig. S1). The weight of MsMOP-Ni and MsMOP-Pt can be stable when heating to 400 °C, losing only 5% of the mass. In comparison, MsMOP-Zn is significantly different from the other polymers, showing one sharp mass loss (10%) at about 340 °C, which may be due to residual final groups of monomer or small molecular weight oligomers.

The formation of polymer framework MsMOPs was confirmed by the Fourier transform infrared (FT-IR) spectra. Fig. S2 showed the FT-IR spectra of MsMOPs and the respective starting materials. MsMOPs remain many feature peaks of their monomers. Such as a strong peak at around 1617 to 1629 cm^{-1}, which is attributed to the stretching of C=N bonds. In addition, the absorbance peaks of MsMOPs exhibit broader than those of the monomers, indicating that the metallosalen monomer is inserted into the polymer networks. Other peaks in the spectra are consistent with the expected network structures. For instance, MsMOP-Ni shows a weak peak at 2250 cm^{-1}, which is attributed to the band of C≡C triple-bond stretching mode of disubstituted acetylene groups. The intense of alkynyl C–H stretching near 3300 cm^{-1} is greatly decreased in MsMOP-Ni, which suggests the possible presence of alkynyl C–H groups in the network. Similar results can be obtained from MsMOP-Zn and MsMOP-Pt. Compared with the corresponding metallosalen monomers, the electronic adsorption spectra of MsMOPs exhibited a long tailing in the low energy region, which showed an extended π-conjugation over the skeleton (Fig. S3).

The chemical structure of MsMOPs was further characterized at molecular level by solid state ^{13}C cross-polarization magic angle spinning nuclear magnetic resonance (^{13}C CP/MAS NMR) spectroscopy. Fig. 1 shows the solid-state ^{13}C NMR spectrum of MsMOP-Ni, the characteristic peaks at 60 ppm and 161 ppm which can be attributed to the carbon atom of methylene and the imine bond in the metallosalen nodes, respectively. Furthermore, a peak of the triple-bonded carbon resonates at around 91 ppm. In addition, the peaks in the range 124 to 151 ppm originate from the carbons atoms of the aromatic rings in the polymer. MsMOP-Zn was also characterized using ^{13}C CP/MAS NMR spectroscopy (Fig. S4), the resonances were similar to those observed in MsMOP-Ni.

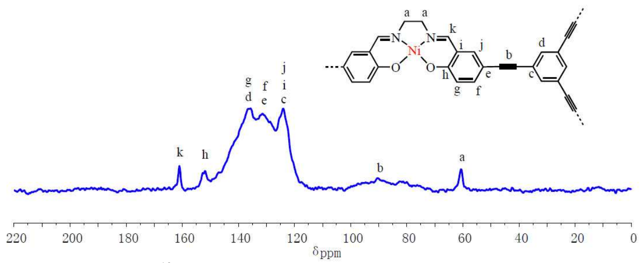

Fig. 1 Solid-state ^{13}C CP/MAS NMR spectra of MsMOP-Ni.

The crystal properties of the MsMOPs were characterized by Powder X-ray diffraction (PXRD) analysis (Fig. S5). The diffraction profiles of MsMOPs did not show any diffraction signals, which indicated that all polymer frameworks have non-order and amorphous structures. Fig. 2 shows the field-emission scanning electron microscopy (FE-SEM) images of the obtained polymers, respectively. The typical SEM images of MsMOP-Ni indicate that the polymer consists of relatively uniform solid submicrometre sphere with particle sizes from 100 to 200 nm. While the samples for MsMOP-Zn and MsMOP-Pt are self-assembled to form larger size particles. In general, the hierarchical morphological feature is unique and interesting particularly for applications in adsorption and catalysis. X-ray photoelectron spectroscopy (XPS) studies were conducted for MsMOPs to characterize the chemical state of the metals (Fig. S6). According to the literatures,19 the Ni, Zn, Pt are present in +2 state. Additionally, Energy dispersive X-ray (EDS) spectra indicate the low residues of catalysts in the polymer framework (Fig. S7).

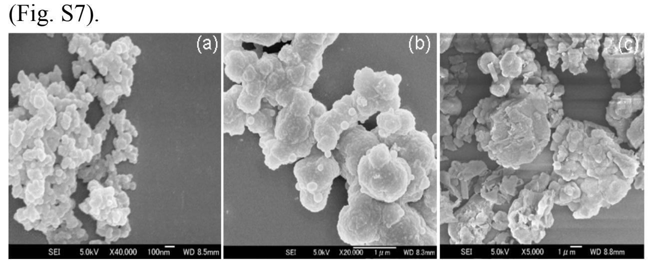

Fig. 2 SEM images of MsMOP-Ni (a), MsMOP-Zn (b) and MsMOP-Pt (c).

Nitrogen sorption analysis was used to analyze the surface area and porous properties of MsMOPs. Fig. 3 shows the nitrogen adsorption-desorption isotherm of three MsMOPs determined at 77 K. MsMOP-Zn has a type-I nitrogen sorption isotherm according to the IUPAC classification and shows a steep nitrogen gas uptake at low relative pressure, indicating that the material is microporous. Compared with MsMOP-Zn, the nitrogen isotherms of MsMOP-Ni and MsMOP-Pt are different at the high pressure region and exhibit a combination of type I and II nitrogen sorption isotherms. With increasing pressure, the nitrogen sorption increases, indicating a high external surface area due to the presence of very small particles. The sharp increase in the nitrogen uptake at a high relative pressure may attribute in part to interparticulate porosity associated with the meso- and macrostructures of the samples. In addition, a small hysteresis can be observed for MsMOP-Ni and MsMOP-Pt based on the isotherms, this phenomenon is associated with the irreversible uptake of gas molecules in the pores. It probably means a swelling in the flexible polymer framework at 77 K by nitrogen.

The pore size calculated from Saito-Flory method shows that all polymer networks have relatively broad pore size distribution (Fig. 4).[5c,18c] The regnant peaks for all MsMOPs apparent at the microspores region (< 2 nm), which agree with the shape of the N_2 sorption isotherm and suggest the present of mainly micropores in all three polymer networks. The important pore data derived from the sorption isotherm such as BET specific surface area, total pore volumes and micropore volumes are listed in Table 1. MsMOP-Pt demonstrates the highest BET surface area in the series of three metallosalen polymer networks. The BET surface area of MsMOP-Pt was calculated to be 1202 m^2g^{-1} in the relative pressure range 0.05-0.20, while MsMOP-Ni and MsMOP-Zn possess BET surface areas of 1087 and 785 m^2g^{-1}, respectively. The BET surface areas of these three MsMOPs are higher than those of MsMOP-1 (554 m^2g^{-1}),[18c] and metallosalen based microporous organic networks (MONs) (522-650 m^2g^{-1}).[18a] The contribution of microporousity of these MsMOPs can be calculated from the ratio of the micropore volume (V_{micro}) over the total pore volume (V_{total}). According to Table 1, the microporosities of MsMOP-Ni, MsMOP-Zn and MsMOP-Pt are around 55%, 54% and 68%, respectively. This indicates that the three metallosalen polymer networks are predominantly microporous.

Table 1 Porosity properties and carbon dioxide uptake for MsMOPs.

Networks	BET surface area $(m^2\ g^{-1})$[a]	Total Pore Volume $(cm^3\ g^{-1})$[b]	Micropore Volume $(cm^3\ g^{-1})$[c]	CO_2 Uptake $(mg\ g^{-1})$[d]	CO_2 Uptake $(mg\ g^{-1})$[e]	Isosteric Heat $(KJ\ mol^{-1})$	CO_2/N_2 Selectivity[f]
MsMOP-Ni	1087	0.780	0.432	81.5	62.6	33.4	46
MsMOP-Zn	785	0.471	0.257	51.6	41.1	26.9	31
MsMOP-Pt	1202	0.938	0.647	73.3	52.9	29.3	20

[a] Calculated from the nitrogen adsorption isotherm using the BET method. [b] Determined from the nitrogen isotherm at $P/P_0 = 0.99$. [c] Determined from the nitrogen isotherm at $P/P_0 = 0.1$. [d] Measured at 1.0 bar and 273 K. [e] Measured at 1.0 bar and 298 K. [f] at 273 K.

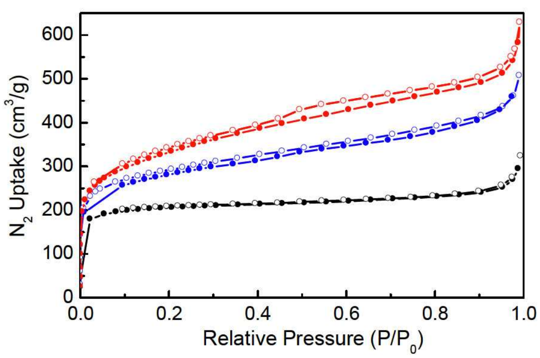

Fig. 3 Nitrogen adsorption-desorption isotherms of MsMOP-Ni (blue line), MsMOP-Zn (black line) and MsMOP-Pt (red line) measured at 77 K. (filled circles: adsorption, open circles: desorption).

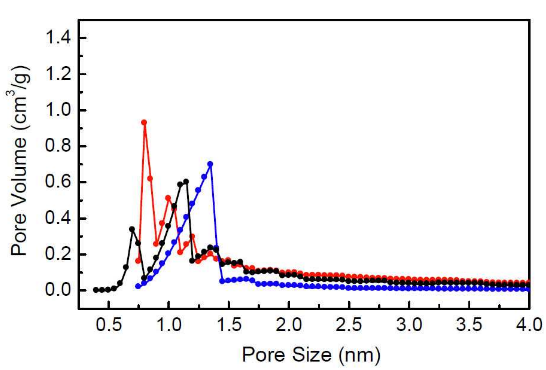

Fig. 4 Pore size distribution of MsMOP-Ni (blue line), MsMOP-Zn (black line) and MsMOP-Pt (red line) calculated by the Saito-Foley method.

The carbon dioxide sorption properties of the three MsMOPs were measured in low pressure at 273 K and 298 K. Fig. 5 shows the carbon dioxide adsorption curves of MsMOPs up to a maximum pressure of 1.0 bar. The MsMOP-Ni exhibits the highest carbon dioxide uptake with 81.5 mg g^{-1}, which is higher than those of reported microporous polymers ACMPs (68.8 mg g^{-1}, at 273 K),[20] conjugated microporous polymer CMP-1-NH_2 (72.2 mg g^{-1}, at 273 K),[12b] borazine-linked polymer BLP-1 (74.0 mg g^{-1}, at 273 K),[21] furan-based imine-linked porous frameworks FOF-1 (77.0 mg g^{-1}, at 273 K),[22] zeolitic imidazolate framework ZIF-100 (74.8 mg g^{-1}, at 273 K)[23] and microporous metal-organic framework SNU-15' (70.0 mg g^{-1}, at 273 K).[24] However, carbon dioxide uptake of MsMOP-Ni is much lower than those of porphyrin based porous organic polymers FePOP-1 (190 mg g^{-1}, at 273 K),[25] *p*-phenylenediamine based porous aromatic framework NPAF (157 mg g^{-1}, at 273 K)[13c] and carbazole-based porous organic polymer CPOP-1 (212 mg g^{-1}, at 273 K).[26] The carbon dioxide uptake of MsMOP-Zn and MsMOP-Pt at 273 K are about 56.1 and 73.3 mg g^{-1}, respectively. Surprisingly, compared with the CO_2 uptake of MsMOP-Pt, MsMOP-Ni has a bigger adsorption capacity, despite MsMOP-Ni exhibits a lower surface area and pore volume. This is possible only because the MsMOP-Ni has a larger microporous distribution, meanwhile the varying unsaturated metal sites in the pore wall of these two frameworks may lead to different interaction between the skeleton and the adsorbate carbon dioxide.[16,27] In addition, these MsMOPs showed high carbon dioxide uptake capacities at 298 K with values 62.3 mg g^{-1} for MsMOP-Ni, 41.1 mg g^{-1} for MsMOP-Zn, and 52.9 mg g^{-1} for MsMOP-Pt, respectively. To get more information of the interaction between MsMOPs and adsorbate carbon dioxide, the isosteric heat of adsorption for carbon dioxide was calculated from the adsorption data collected at 273 and 298 K using the Clausius-Clapeyron equation.[28] The isosteric heat for carbon dioxide determined at low loading was 33.4 kJ mol^{-1} for MsMOP-Ni, which higher than 26.9 kJ mol^{-1} for MsMOP-Zn, and 29.3 kJ mol^{-1} for MsMOP-Pt (Fig. 5). We presumed that not only the porosity of the microporous organic polymers with metallosalen units determines their isosteric heat, but also the different unsaturated metal sites are an important factor.[29] These values are higher than the results of reported HCP materials[30] and triptycene-based microporous poly(benzimidazole) networks TBIs,[31] comparable with microporous cyanate resins[32] and inorganic-organic hybrid porous polymers (HPPs)[33], but lower than the amine functionalized POPs.[14b] The selective separation of CO_2 is very important in that it could give a clean and durable energy supply by control of disasterous carbon dioxide molecules. Once the porosity and CO_2 uptake properties of MsMOPs were researched, we considered their performance in selective CO_2 capture over N_2 for potential use in gas separation applications. The adsorption isotherms of N_2 at 273 K were measured and are compared with that of CO_2 in Fig. S8. The curves display that CO_2 has the considerably higher uptake than N_2 in the whole pressure range. On the basis of initial slope calculations in the pressure range of 0 to 0.1 bar, the ideal adsorption selectivity of CO_2/N_2 is 46 for MsMOP-Ni, 31 for MsMOP-Zn, and 20 for MsMOP-Pt, respectively. Although the values are lower than those of reported MOPs,[13a,34] they are comparable to many other types of polymers including PCTFs,[35a] CTFs,[6c] MOPs,[35b]etc.

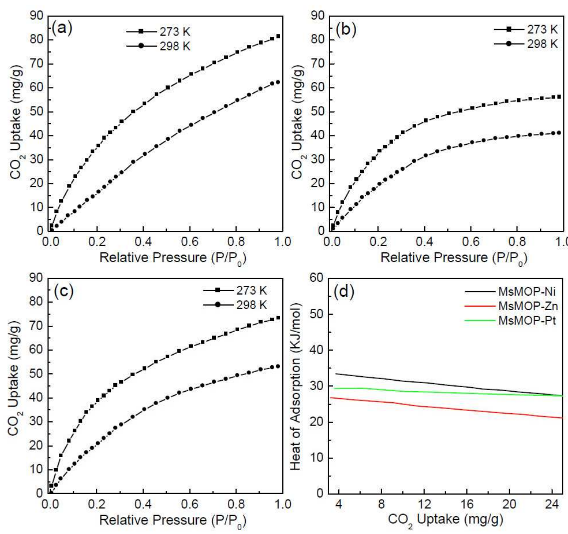

Fig. 5 CO_2 adsorption isotherm at 273 and 298 K of MsMOP-Ni (a), MsMOP-Zn (b), MsMOP-Pt (c) and their adsorption heat (d).

Conclusions

In summary, three novel porous organic polymer frameworks with built-in metal sites were successfully prepared by Sonogashira-Hagihara cross-coupling reaction using different metallosalen as a key building block. The new porous materials are insoluble in common organic solvents or water, and can keep stable up to 300 °C under nitrogen atmosphere. It was found that their porosity was effected by different metallosalen building blocks. These materials possess good carbon dioxide storage properties in low pressure, the differences of the uptake capacity and adsorption heat for carbon dioxide between MsMOPs indicated the unsaturated metal sites in the framework can impact on the interaction between the adsorbate and skeleton. Especially, using this synthetic strategy we can easily prepare homochiral porous organic polymer framework with single catalytic center using chiral metallosalen as comonomer. Currently, research into the asymmetric catalytic properties of homochiral metallosalen porous organic polymer framework as heterogeneous catalyst are underway in our laboratory.

Experimental

Materials

All cross linking reactions were operated using the standard Schlenk line techniques. 1,3,5-Triethynylbenzene, tetrakis(triphenylphosphine)palladium(0) and copper(I) iodide were purchased from Aldrich and used as received. Organic solvents for reactions were distilled over appropriate drying reagents under nitrogen. Deuterated solvents for NMR measurement were obtained from Aldrich.

Instrumentation

^1H NMR spectra were recorded on a JEOL model JNM-LA400 NMR spectrometer, where the chemical shifts (δ in ppm) were determined with a residual proton of the solvent as standard. Solid-state ^{13}C CP/MAS NMR measurements were recorded on a Bruker AVANCE III 400 WB spectrometer at a MAS rate of 5 kHz and a CP contact time of 2 ms. ^{13}C CP MAS chemical shifts are referenced to the resonances of adamantane ($C_{10}H_{16}$) standard (δ CH_2 = 38.5). The infrared spectra were recorded from 400 to 4000 cm^{-1} on a Nicolet FT-IR 360 spectrometer by using KBr pellets. UV-vis absorption spectra were recorded on a Shimadzu UV-2550 spectrophotometer. Elemental analyses were carried out on an Elementar model vario EL cube analyzer. Field emission scanning electron microscopy was performed on a JEOL model JEM-6700 microscope operating at an accelerating voltage of 5.0 kV. X-ray diffraction (XRD) data were recorded on a Rigaku model RINT Ultima III diffractometer by depositing powder on glass substrate, from 2θ = 1.5° up to 60° with 0.02° increment. Thermogravimetric analysis (TGA) was performed on a TA Q500 thermogravimeter by measuring the weight loss while heating at a rate of 10 °C min^{-1} from 25 to 800 °C under nitrogen. X-ray photoelectron spectroscopy (XPS) was performed using an ESCALAB 250 spectrometer. Nitrogen and carbon dioxide sorption isotherms were measured using a JW-BK 132F analyzer. Before measurement, the samples were degassed in vacuum at 150 °C for more than 10 h. The Brunauer-Emmett-Teller (BET) method was utilized to calculate the specific surface areas and pore volume, the Saito-Foley (SF) method was applied for the estimation of pore size distribution.

Synthesis of MsMOPs

All of the metallosalen porous organic polymers (MsMOPs) were synthesized by palladium catalyzed Sonogashira-Hagihara cross-coupling polycondensation of 1,3,5-triethynylbenzene and corresponding metallosalen monomer. All reactions were carried out using a 1.5 M excess of the 1,3,5-triethynylbenzene since this found to maximize surface areas in the microporous polymer frameworks. A typical experimental procedure for MsMOP-Ni is given in details as follows: 1,3,5-Triethynylbenzene (30.1 mg, 0.2 mmol), Salen-Ni (60.0 mg, 0.13 mmol), were dissolved in THF (6.0 mL) and triethylamine (6.0 mL), and then the mixture was degassed by the freeze-pump-thaw cycles. To the mixture were added tetrakis(triphenylphosphine)palladium(0) (16.2 mg, 0.014 mmol) and copper(I) iodide (4.0 mg, 0.02 mmol). The resulting mixture was heated to 80 °C and stirred for 72 h under a nitrogen atmosphere. After cooled to room temperature, the precipitate was filtered and washed three times with water, chloroform, methanol and acetone to remove any unreacted monomer and catalyst. Further purification of the target polymer was carried out by Soxhlet extraction with water, methanol, and tetrahydrofuran for 48 h. The target product was dried at 150 °C under vacuum for 24 h to give 51.3 mg (yield = 84.6%) polymers. All MsMOPs were isolated as brown powders with similar isolation yield 81.8% for MsMOP-Zn and 86.2% for MsMOP-Pt).

Acknowledgements

This work was supported by the National Natural Science Foundation of China (Nos.: 51203058, 51373064, 51173061 and 21074043). X. Liu is also grateful for support by the Frontiers of Science and Interdisciplinary Innovation Project of Jilin University (No.: 450060481015).

Notes and references

[a] *State Key Laboratory for Supramolecular Structure and Materials, College of Chemistry, Jilin University, 2699 Qianjin Avenue, Changchun, 130012, P.R.China. E-mail: xm_liu@jlu.edu.cn*
[b] *State Key Laboratory on Integrated Optoelectronics, College of Electronic Science and Technology, Jilin University, Changchun, 130012, P.R.China.*
[c] *State Key Laboratory of Inorganic Synthesis and Preparative Chemistry, College of Chemistry, Jilin University, Changchun, 130012, P.R.China.*

† Electronic Supplementary Information (ESI) available: TGA, FT-IR, UV spectra, PXRD, XPS, EDS spectra of MsMOPs and ^{13}C CP/MAS NMR spectra of MsMOP-Zn, ^{1}H-NMR spectra of monomers. see DOI: 10.1039/b000000x/

1 (a) R. S. Haszeldine, *Science*, 2009, **325**, 1647; (b) D. M. D'Alessandro, B. Smit and J. R. Long, *Angew. Chem. Int. Ed.*, 2010, **49**, 6058; (c) S. A. Montzka, E. J. Dlugokencky and J. H. Butler, *Nature*, 2011, **476**, 43; (d) R. Monastersky, *Nature*, 2013, **497**, 13.
2 (a) S. Keskin, T. M. van Heest and D. S. Sholl, *ChemSusChem*, 2010, **3**, 879; (b) G. Férey, C. Serre, T. Devic, G. Maurin, H. Jobic, P. L. Llewellyn, G. D. Weireld, A. Vimont, M. Daturi and J. Chang, *Chem. Soc. Rev.*, 2011, **40**, 550; (c) J. Liu, P. K. Thallapally, B. P. McGrail, D. R. Brown and J. Liu, *Chem. Soc. Rev.*, 2012, **41**, 2308; (d) M. M. F. Hasan, E. L. First and C. A. Floudas, *Phys. Chem. Chem. Phys.*, 2013, **15**, 17601.
3 (a) N. B. McKeown and P. M. Budd, *Chem. Soc. Rev.*, 2006, **35**, 675; (b) N. Du, H. B. Park, G. P. Robertson, M. M. Dal-Cin, T. Visser, L. Scoles and M. D. Guiver, *Nat. Mater.*, 2011, **10**, 372; (c) M. Carta, R. Malpass-Evans, M. Croad, Y. Rogan, J. C. Jansen, P. Bernardo, F. Bazzarelli and N. B. McKeown, *Science*, 2013, **339**, 303.
4 (a) C. D. Wood, B. Tan, A. Trewin, H. Niu, D. Bradshaw, M. J. Rosseinsky , Y. Z. Khimyak, N. L. Campbell, R. Kirk, E. Stoeckel and A. I. Cooper, *Chem. Mater.*, 2007, **19**, 2034; (b) M. G. Schwab, A. Lennert, J. Pahnke, G. Jonschker, M. Koch, I. Senkovska, M. Rehahn and S. Kaskel, *J. Mater. Chem.*, 2011, **21**, 2131; (c) S. Xu, Y. Luo and B. Tan, *Macromol. Rapid Commun.*, 2013, **34**, 471.
5 (a) X. Liu, Y. Zhang, H. Li, S. A, H. Xia and Y. Mu, *RSC Adv.*, 2013, **3**, 21267; (b) X. Liu, Y. Xu, Z. Guo, A. Nagai and D. Jiang, *Chem. Commun.*, 2013, **49**, 3233; (c) X. Liu, Y. Xu and D. Jiang, *J. Am. Chem. Soc.*, 2012, **134**, 8738; (d) Y. Xu, S. Jin, H. Xu, A. Nagai and D. Jiang, *Chem. Soc. Rev.*, 2013, **42**, 8012; (e) S. A, Y. Zhang, Z. Li, H. Xia, M. Xue, X. Liu and Y. Mu, *Chem. Commun.*, 2014, **50**, 8495; (e) Y. Zhang, S. A, Y. Zou, X. Luo, Z. Li, H. Xia, X. Liu and Y. Mu, *J. Mater. Chem. A,*2014, DOI: 10.1039/C4TA01871K.
6 (a) P. Kuhn, M. Antonietti and A. Thomas, *Angew. Chem. Int. Ed.*, 2008, **47**, 3450; (b) P. Kuhn, A. Forget, J. Hartmann, A. Thomas and M. Antonietti, *Adv. Mater.*, 2009, **21**, 897; (c) S. Ren, M. J. Bojdys, R. Dawson, A. Laybourn, Y. Z. Khimyak, D. J. Adams and A. I. Cooper, *Adv. Mater.*, 2012, **24**, 2357; (d) X. Liu, H. Li, Y. Zhang, B. Xu, S. A, H. Xia and Y. Mu, *Polym. Chem.*, 2013, **4**, 2445.
7 (a) A. P. Cote, A. I. Benin, N. W. Ockwig, M. O'Keeffe, A. J. Matzger and O. M. Yaghi, *Science*, 2005, **310**, 1166; (b) H. M. El-Kaderi, J. R. Hunt, J. L. Mendoza-Cortes, A. P. Cote, R. E.Taylor, M. O'Keeffe and O. M. Yaghi, *Science*, 2007, **316**, 268; (c) X. Feng, X. Ding and D. Jiang, *Chem. Soc. Rev.*, 2012, **41**, 6010; (d) J. W. Colson and W. R. Dichtel, *Nature Chem.*, 2013, **5**, 453; (e) S. Ding and W. Wang, *Chem. Soc. Rev.*, 2013, **42**, 548.
8 (a) R. Dawson, A. I. Cooper and D. J. Adams, *Prog. Polym. Sci.*, 2012, **37**, 530; (b) F. Vilela, K. Zhang and M. Antonietti, *Environ. Sci.*, 2012, **5**, 7819; (c) Z. Chang, D. Zhang, Q. Chen and X. Bu, *Phys. Chem. Chem. Phys.*, 2013, **15**, 5430; (d) D. Wang, W. Yang, L. Li, X. Zhao, S. Feng and H. Liu, *J. Mater. Chem. A*, 2013, **1**, 13549; (e) Y. Wu, D. Wang, L. Li, W. Yang, S. Feng and H. Liu, *J. Mater. Chem. A*, 2014, **2**, 2160.
9 (a) K. V. Rao, S. Mohapatra, T. K. Maji and S. J. George, *Chem. Eur. J.*, 2012, **18**, 4505; (b) C. Gu, N. Huang, J. Gao, F. Xu, Y. Xu and D. Jiang, *Angew. Chem. Int. Ed.*, 2014, **53**, 1.
10 (a) L. Chen, Y. Yang and D. Jiang, *J. Am. Chem. Soc.*, 2010, **132**, 9138; (b) P. Kaur, J. T. Hupp and S. T. Nguyen, *ACS Catal.*, 2011, **1**, 819; (c) Y. Zhang and S. N. Riduan, *Chem. Soc. Rev.*, 2012, **41**, 2083; (d) X. Liu, S. A, Y. Zhang, X. Luo, H. Xia, H. Li and Y. Mu, *RSC Adv.*, 2014, **4**, 6447.
11 (a) S. Ren, R. Dawson, A. Laybourn, J. Jiang, Y. Khimyak, D. J. Adams and A. I. Cooper, *Polym. Chem.*, 2012, **3**, 928; (b) M. R. Liebl and J. Senker, *Chem. Mater.*, 2013, **25**, 970.
12 (a) R. Vaidhyanathan, S. S. Iremonger, G. K. H. Shimizu, P. G. Boyd, S. Alavi and T. K. Woo, *Science*, 2010, **330**, 650; (b) R. Dawson, D. J. Adams and A. I. Cooper, *Chem. Sci.*, 2011, **2**, 1173; (c) W. Lu, J. P. Sculley, D. Yuan, R. Krishna, Z. Wei and H. C. Zhou, *Angew. Chem. Int. Ed.*, 2012, **51**, 7480; (d) L. H. Xie and M. P. Suh, *Chem. Eur. J.*, 2013, **19**, 11590.
13 (a) M. G. Rabbani and H. M. El-Kaderi, *Chem. Mater.*, 2012, **24**, 1511; (b) E. Preis, C. Widling, G. Brunklaus, J. Schmidt, A. Thomas and U. Scherf, *ACS Macro. Lett.*, 2013, **2**, 380; (c) D. E. Demirocak, M. K. Ram, S. S. Srinivasan, D. Y. Goswami and E. K. Stefanakos, *J. Mater. Chem. A*, 2013, **1**, 13800; (d) S. Qiao, Z. Du and R. Yang, *J. Mater. Chem. A*, 2014, **2**, 1877.
14 (a) A. P. Katsoulidis and M. G. Kanatzidis, *Chem. Mater.*, 2011, **23**, 1818; (b) V. Guillerm, Ł. J. Weseliński, M. Alkordi, M. I. H. Mohideen, Y. Belmabkhout, A. J. Cairns and M. Eddaoudi, *Chem. Comm.*, 2014, **50**, 1937.
15 H. Ma, H. Ren, X. Zou, S. Meng, F. Sun and G. Zhu, *Polym. Chem.*, 2014, **5**, 144.
16 P. Mishra, S. Edubilli, B. Mandal and S. Gumma, *J. Phys. Chem. C*, 2014, **118**, 6847.
17 (a) P. G. Cozzi, *Chem. Soc. Rev.*, 2004, **33**, 410; (b) C. Baleizão and H. Garcia, *Chem. Rev.*, 2006, **106**, 3987; (c) S. J. Wezenberg and A. W. Kleij, *Angew. Chem. Int. Ed.*, 2008, **47**, 2354.
18 (a) J. Chun, S. Kang, N. Kang, S. M. Lee, H. J. Kim and S. U. Son, *J. Mater. Chem. A*, 2013, **1**, 5517; (b) Y. Xie, T. Wang, X. Liu, K. Zou and W. Deng, *Nat. Commun.*, 2013, **4**, 1960; (c) H. Li, B. Xu, X. Liu, S. A, C. He, H. Xia and Y. Mu, *J. Mater. Chem. A*, 2013, **1**, 14108.
19 (a) Y. Shimazaki, T. Yajima, F. Tani, S. Karasawa, K. Fukui, Y. Naruta and O. Yamauchi, *J. Am. Chem. Soc.*, 2007, **129**, 2559; (b) M. Salavati-Niasari, F. Davar and A. Khansari, *J. Alloys Compd.*, 2011, **509,** 61.
20 J. H. Choi, K. M. Choi, H. J. Jeon, Y. J. Choi, Y. Lee and J. K. Kang, *Macromolecules*, 2010, **43**, 5508.
21 K. T. Jackson, M. G. Rabbani, T. E. Reich and H. E. El-Kaderi, *Polym. Chem.*, 2011, **2**, 2775.
22 J. Ma, M. Wang, Z. Du, C. Chen, J. Gao and J. Xu, *Polym. Chem.*, 2012, **3**, 2346.
23 B. Wang, A. P. Cote, H. Furukawa, M. O'Keeffe and O. M. Yaghi, *Nature*, 2008, **453**, 207.
24 Y. E. Cheon and M. P. Suh, *Chem. Commun.*, 2009, 2296.
25 A. Modak, M. Nandi, J. Mondal and A. Bhaumik, *Chem. Commun.*, 2012, **48**, 248.
26 Q. Chen, M. Luo, P. Hammershoj, D. Zhou, Y. Han, B. W. Laursen, C. G. Yan and B. H. Han, *J. Am. Chem. Soc.*, 2012, **134**, 6084.
27 (a) C. R. Wade and M. Dincă, *Dalton Trans.*, 2012, **41**, 7931; (b) H. J. Park and M. P. Suh, *Chem. Sci.*, 2013, **4**, 685.
28 (a) Y. S. Bae and R. Q. Snurr, *Angew. Chem. Int. Ed.*, 2011, **50**, 11586; (b) K. Sumida, D. L. Rogow, J. A. Mason, T. M. Mcdonald, E. D. Bloch, Z. R. Herm, T. H. Bae and J. R. Long, *Chem. Rev.*, 2012, **112**, 724.
29 Z. Zhang, W. Y. Gao, L. Wojtas, S. Ma, M. Eddaoudi and M. J. Zaworotko, *Angew. Chem. Int. Ed.*, 2012, **51**, 9330.
30 C. F. Martin, E. Stöckel, R. Clowers, D. J. Adams, A. I. Cooper, J. J. Pis, F. Rubiera and C. J. pevida, *J. Mater. Chem.*, 2011, **21**, 5475.
31 H. Lim, M. C. Cha and J. Y. Chang, *Macromol. Chem. Phys.*, 2012, **213**, 1385.

32 (a) H. Yu, C. Shen, M. Tian, J. Qu and Z. Wang, *Macromolecules*, 2012, **45**, 5140; (b) H. Yu, C. Shen, M. Tian, J. Qu and Z. Wang, *ChemPlusChem*, 2013, **78**, 498.
33 D. Wang, W. Yang, S. Feng and H. Liu, *Polym. Chem.*, 2014, **5**, 3634.
34 (a) H. A. Patel, S. H. Je, J. Park, Y. Jung, A. Coskun and C. T. Yavuz, *Chem. Eur. J.,* 2014, **20**, 772; (b) P. Mohanty, L. D. Kull and K. Landskron, *Nat. Commun.,* 2011, **2**, 401; (c) M. G. Rabbani, A. K. Sekizkardes, O. M. El-Kadri, B. R. Kaafarani and H. M. El-Kaderi, J. *Mater. Chem.,* 2012, **22**, 25409.
35 (a) A. Bhunia, I. Boldog, A. Moller and C. Janiak, *J. Mater. Chem. A*, 2013, **1**, 14990; (b) R. Dawson, E. Stockel, J. R. Holst, D. J. Adams and A. I. Cooper, *Energy Environ. Sci.*, 2011, **4**, 4239.

Three metallosalen-based microporous organic polymers were designed and synthesized. New materials display excellent porosity and good capacities for store and separation of carbon dioxide at 273 K and 1 bar.